Statistical entropy of a binary hard-sphere mixture: the low-density limit

1996 J. Phys.: Condens. Matter 8 8137

(http://iopscience.iop.org/0953-8984/8/43/010)

J. Phys.: Condens. Matter **8** (1996) 8137–8144. Printed in the UK

Statistical entropy of a binary hard-sphere mixture: the low-density limit

F Saija and P V Giaquinta†

Istituto Nazionale per la Fisica della Materia and Università degli Studi di Messina, Dipartimento di Fisica, CP 50, 98166 S Agata-Messina, Italy

Received 18 June 1996, in final form 12 August 1996

Abstract. We have studied the virial expansion of the configurational entropy of a binary mixture of unequal hard spheres as a function of the diameter ratio and of the relative concentration of the two species. The entropy was analysed as a sum of two terms: a pair term, which arises from two-particle spatial correlations, and a residual contribution that is associated with correlations involving more than two particles. We discuss the behaviour of this last quantity in the regime of strongly asymmetric sizes and concentrations with specific regard to the onset of the mechanism leading to phase separation at a thermodynamic level.

1. Introduction

The thermodynamic stability of fluid mixtures and, in particular, the problem of phase segregation are currently subjects of great experimental interest [1, 2]. On the theoretical side, the occurrence of a demixing transition in a binary mixture has been demonstrated for some rather simplified lattice and continuum models with barely repulsive interactions as the result of purely entropic effects which play a crucial role in the regime of highly asymmetric sizes and concentrations [3–6]. The behaviour of a two-component mixture composed of unequal hard spheres has been also analysed through a variety of approximate theoretical techniques including integral-equation theories [7, 8], density-functional methods [9], and other approaches [10, 11]. However, a definite assessment on this question is still lacking because of the absence of reliable numerical simulation results in the regime that is relevant for the onset of the phenomenon [12–14].

Recently, we have studied the configurational entropy of a binary hard-core mixture in the fluid phase in the Percus–Yevick (PY) approximation [15]. This type of analysis was carried out by explicitly calculating the contribution which arises from two-particle correlations. In this regard, we found rather unambiguous interrelations between the transitions undergone by the mixture (i.e., freezing, phase separation) and the thermodynamic behaviour of the residual multiparticle entropy Δs. This quantity is obtained from the total entropy of the fluid after subtraction of a (qualitatively uninteresting) background value that is calculated as the sum of the ideal and pair terms, and displays a nonmonotic behaviour as a function of the total packing fraction. We noted that the crossover undergone by Δs from negative to positive values is a rather sensitive indicator of the structural changes which take place in the system on a local scale. In particular, when the size ratio of the two species is not very far from one, the ordering threshold traced through this one-phase

† Author to whom any correspondence should be addressed; e-mail: giaquint@vulcano.unime.it.

0953-8984/96/438137+08$19.50

entropic criterion is in fairly good agreement with the available simulation data for the freezing point of the mixture. In the opposite regime of very different diameters and, more specifically, for values of the size ratio less than about 0.2, the locus of the points where Δs vanishes has a very different behaviour as a function of the relative concentration, dropping below the freezing threshold of the pure fluid. We surmised that this fact signals the onset in the system of a new type of order and noted also that a better resolution at very low concentrations would call for an analytical expansion of the theory to be carried out in the limit of very small packing fractions.

In this paper we present such an expansion that is pushed up to a level which corresponds to the virial expansion of the pressure truncated at the fourth order in the density [16, 17].

2. Virial expansion of the statistical entropy

The total excess entropy of a multicomponent system can be expressed as an infinite series:

$$s^{(ex)} = \sum_{n=2}^{\infty} s_n \tag{1}$$

where $s^{(ex)}$ is the excess entropy per particle in units of the Boltzmann constant, and the partial entropies s_n are obtained from the integrated contributions of the spatial correlations between n-tuples of particles. In particular, the two-body term can be written as [15]

$$s_2 = -\frac{1}{2}\rho \sum_{ij} x_i x_j \int \left\{ g_{ij}(r) \ln\left[g_{ij}(r)\right] - g_{ij}(r) + 1 \right\} \mathrm{d}\boldsymbol{r} \tag{2}$$

where $\rho = \rho_1 + \rho_2$ is the total number density, x_i is the mole fraction of species i $(i = 1, 2)$, and the quantities $g_{ij}(r)$ are the partial pair distribution functions. The residual multiparticle entropy

$$\Delta s \equiv s^{(ex)} - s_2 \tag{3}$$

despite its minor quantitative relevance in the overall balance, turns out to be a rather sensitive indicator of the structural and dynamical changes which take place in the system [15]. For a mixture composed of hard-core particles with diameters σ_i, the exclusion terms in equation (2) can be integrated out to give

$$s_2(\rho, x_1) = -B(x_1)\rho - 2\pi\rho \sum_{ij} x_i x_j \int_{\sigma_{ij}}^{\infty} \left\{ g_{ij}(r) \ln\left[g_{ij}(r)\right] - g_{ij}(r) + 1 \right\} r^2 \, \mathrm{d}r \tag{4}$$

where

$$B(x_1) = \frac{2}{3}\pi x_1^2 \sigma_{11}^3 + \frac{4}{3}\pi x_1 (1 - x_1)\sigma_{12}^3 + \frac{2}{3}\pi (1 - x_1)^2 \sigma_{22}^3 \tag{5}$$

is the second-order virial coefficient of the mixture and $\sigma_{ij} = (\sigma_i + \sigma_j)/2$. In the following, we denote the diameter ratio as $\mathcal{R} = \sigma_2/\sigma_1 \leqslant 1$.

The expansion of the total excess entropy that is obtained after integration of the compressibility factor yields at third order in the density

$$s^{(ex)}(\rho, x_1) = -B(x_1)\rho - \frac{1}{2}C(x_1)\rho^2 - \frac{1}{3}D(x_1)\rho^3 + \cdots \tag{6}$$

where $C(x_1)$ and $D(x_1)$ are the third-order and fourth-order virial coefficients, respectively [16, 17].

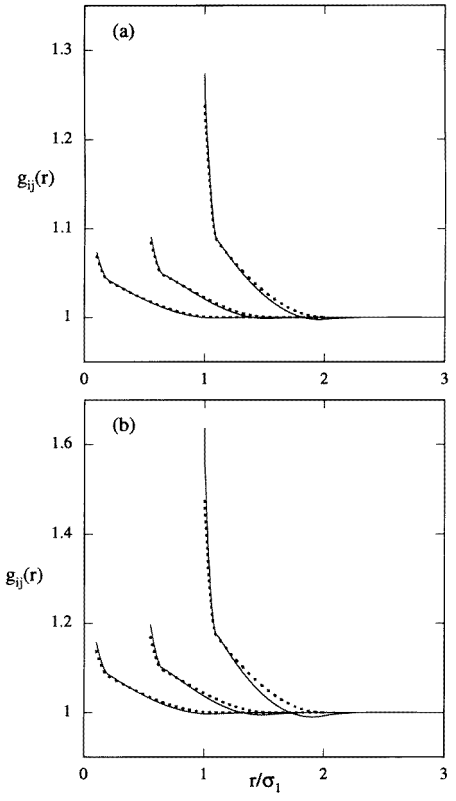

Figure 1. Radial distribution functions $g_{ij}(r)$, plotted as functions of r/σ_1 for $\mathcal{R} = 0.1$, $x_1 = 5\times10^{-3}$ and for two values of the total packing fraction: (a) $\eta = 0.05$; (b) $\eta = 0.1$. The dotted curves refer to the low-density expansion, while the continuous curves represent the Percus–Yevick results.

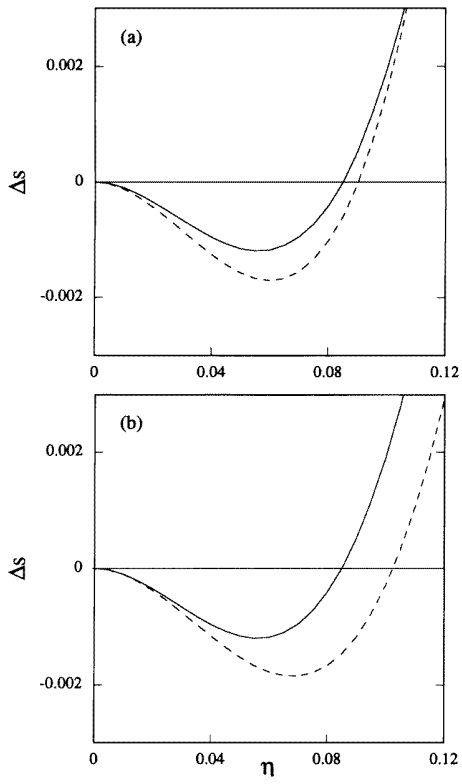

Figure 2. Residual multiparticle entropy $\Delta s(\eta, x_1; \mathcal{R})$ plotted as a function of the total packing fraction η for $\mathcal{R} = 0.1$ and for two values of the larger-particle mole fraction: (a) $x_1 = 5 \times 10^{-3}$; (b) $x_1 = 1 \times 10^{-2}$. The dotted curves refer to the low-density expansion, while the continuous curves represent the Percus–Yevick results.

As far as the 'pair' entropy s_2 is concerned, we expand the radial distribution functions $g_{ij}(r)$ of the mixture in powers of the density as [18]

$$g_{ij}(r) = 1 + \mathrm{e}^{-\beta u_{ij}(r)} \sum_{n=1}^{\infty} \rho^n g_{ij}^{(n)}(r) \tag{7}$$

where $u_{ij}(r)$ is the pair interaction potential for the interaction between two particles of species i and j, respectively, and β is the inverse temperature in units of the Boltzmann constant. The first-order contributions to the pair distribution functions $g_{ij}^{(1)}(r)$ are evaluated explicitly for a binary hard-sphere mixture in the appendix. After using equation (7) in the expansion of the integrand which appears in equation (4), we obtain at second order in the density

$$g_{ij}(r)\ln\bigl[g_{ij}(r)\bigr] - g_{ij}(r) + 1 = \frac{1}{2}\bigl[g_{ij}^{(1)}(r)\bigr]^2\rho^2 + \cdots \tag{8}$$

where the first-order term is found to vanish exactly. Using equations (A2)–(A4), the density

expansion of s_2 pushed to third order in ρ reads

$$s_2(\rho, x_1) = -B(x_1)\rho - \pi K(x_1)\rho^3 + \cdots \tag{9}$$

where

$$\begin{aligned} K(x_1) = {} & x_1^4 \int_{\sigma_{11}}^{2\sigma_{11}} \Big[\mathcal{A}(r)\Big]^2 r^2 \, \mathrm{d}r + 2x_1^3(1-x_1) \int_{\sigma_{12}}^{2\sigma_{12}} \Big[\mathcal{A}(r)\mathcal{C}(r)\Big] r^2 \, \mathrm{d}r \\ & + x_1^2(1-x_1)^2 \int_{\sigma_{12}}^{2\sigma_{12}} \Big[\mathcal{C}(r)\Big]^2 r^2 \, \mathrm{d}r + x_1^2(1-x_1)^2 \int_{\sigma_{12}}^{2\sigma_{12}} \Big[\mathcal{C}(r)\Big]^2 r^2 \, \mathrm{d}r \\ & + 2x_1(1-x_1)^3 \int_{\sigma_{22}}^{2\sigma_{12}} \Big[\mathcal{B}(r)\mathcal{C}(r)\Big] r^2 \, \mathrm{d}r + (1-x_1)^4 \int_{\sigma_{22}}^{2\sigma_{22}} \Big[\mathcal{B}(r)\Big]^2 r^2 \, \mathrm{d}r \\ & + 2x_1^3(1-x_1) \int_{\sigma_{12}}^{\sigma_{11}+\sigma_{12}} \Big[\mathcal{D}(r)\Big]^2 r^2 \, \mathrm{d}r \\ & + 4x_1^2(1-x_1)^2 \int_{\sigma_{12}}^{\sigma_{12}+\sigma_{22}} \Big[\mathcal{D}(r)\mathcal{E}(r)\Big] r^2 \, \mathrm{d}r \\ & + 2x_1(1-x_1)^3 \int_{\sigma_{12}}^{\sigma_{12}+\sigma_{22}} \Big[\mathcal{E}(r)\Big]^2 r^2 \, \mathrm{d}r. \end{aligned} \tag{10}$$

The quantities $\mathcal{A}(r)$, $\mathcal{B}(r)$, $\mathcal{C}(r)$, $\mathcal{D}(r)$, and $\mathcal{E}(r)$ are defined in the appendix. After combining equation (6) with equation (9), we obtain

$$\Delta s(\rho, x_1) = -\frac{1}{2} C(x_1)\rho^2 - \frac{1}{3}\Big[D(x_1) - 3\pi K(x_1)\Big]\rho^3 + \cdots. \tag{11}$$

In the limit where $x_1 = 1$, equation (11) consistently reduces to the homologous expression for the one-component case [19].

3. Results

Figure 1 shows the pair distribution functions of the mixture in the low-density asymmetric regime. The $g_{ij}(r)$s are computed through the first-order virial expansion for $\mathcal{R} = 0.1$, the larger-particle mole fraction $x_1 = 5 \times 10^{-3}$, and for two values of the total packing fraction $\eta = \frac{1}{6}\pi\rho(x_1\sigma_1^3 + x_2\sigma_2^3)$. The first-order expansions are then compared with the corresponding quantities evaluated in the PY approximation after Fourier inverting the analytical expressions for the partial structure factors. The resulting functions were calculated over a range of 30 large-sphere diameters with a spatial resolution $\Delta r/\sigma_1 \simeq 3 \times 10^{-5}$ in order to obtain reliable estimates also for the residual multiparticle entropy.

The behaviour of $\Delta s(\eta, x_1; \mathcal{R})$ as a function of η is then shown for $\mathcal{R} = 0.1$ in figure 2 for two values of x_1. We note that in this range of the parameters the first-order approximation for Δs is qualitatively consistent with the corresponding PY estimate.

The locus of points $\eta_0(x_1; \mathcal{R})$ where the residual multiparticle entropy vanishes is shown in figure 3 for five values of the diameter ratio. We remark that, by construction, this quantity conveys reliable information only in a range of low enough total densities. The behaviour for x_1 approaching both zero and one is thus manifestly unphysical. For comparison, we also show some data obtained with the PY approximation for $\mathcal{R} = 0.1$. These data confirm that the functional behaviour of Δs as a function of the concentration is already correctly embodied in the density expansion truncated at the third order. Similar results have been recently obtained with a different integral closure [8].

A sharp change of behaviour in the compositional dependence of $\eta_0(x_1; \mathcal{R})$ was already observed for $\mathcal{R} \lesssim 0.2$ in [15], where the authors noticed that, for such values of the diameter

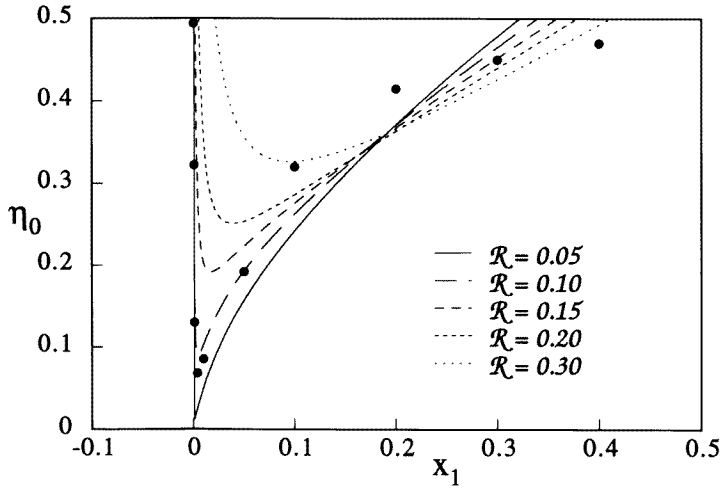

Figure 3. The locus of points $\eta_0(x_1;\mathcal{R})$ where $\Delta s(\eta, x_1;\mathcal{R}) = 0$, plotted as a function of the larger-particle mole fraction x_1 for five values of the size ratio. The solid circles represent the Percus–Yevick results for $\mathcal{R} = 0.10$.

ratio, this function lay below the 'pure' hard-sphere freezing point over a rather wide composition range. This circumstance is confirmed by the present results even in the regime of very dilute concentrations of the larger-sphere component. In fact, as seen from figure 3, upon adding larger particles onto a solvent formed by the smaller spheres, the ordering threshold that is monitored through the zero of Δs initially drops down to lower and lower values of the total packing fraction. This behaviour indicates that, when the concentration of the larger-sphere component is very small, the local structural mechanism that was originally responsible for the freezing of the formerly pure solvent fluid is sensitively affected by the presence of the solute. As a result, the ordering threshold is pushed toward a range of densities where one can safely exclude the solidification of the mixture as a whole. This trend inverts at a rather small value of the concentration ($x_1^{(min)} \simeq 5 \times 10^{-3}$ for $\mathcal{R} = 0.1$) beyond which the curve starts rising again. The ensuing minimum in $\eta_0(x_1;\mathcal{R})$ becomes sharper and deeper as the size difference between the two species increases, while shifting to lower values of x_1. It thus follows that in a strongly asymmetric mixture whose concentration is close to that which corresponds to the minimum, the range of total packing fractions within which Δs is negative reduces dramatically (see figure 2).

The clear indication of two distinct structural regimes which emerges from figure 3 (corresponding, respectively, to concentrations lower or greater than $x_1^{(min)}$) is consistent with a recent study of the virial equation of state of the mixture expanded up to the fifth order in the density [20]. In particular, the negative deviation of the fifth-order virial expansion from the 'reference' BMCSL equation of state which was proposed by Boublík [21] and by Mansoori, Carnahan, Starling, and Leland [22] is found to be maximal, for an assigned value of the size ratio, in the same region of concentrations.

The identification of the two regimes is also evident in a representation of the data where the smaller-sphere packing fraction η_2 is plotted as a function of η_1, each pair (η_1, η_2) corresponding to a point of the curve $\eta_0(x_1;\mathcal{R})$. In figure 4, states of constant mole fraction lie on straight lines which radiate from the origin, while states of constant total packing fraction form lines which intersect both axes at 45°. We also note that, for an assigned value

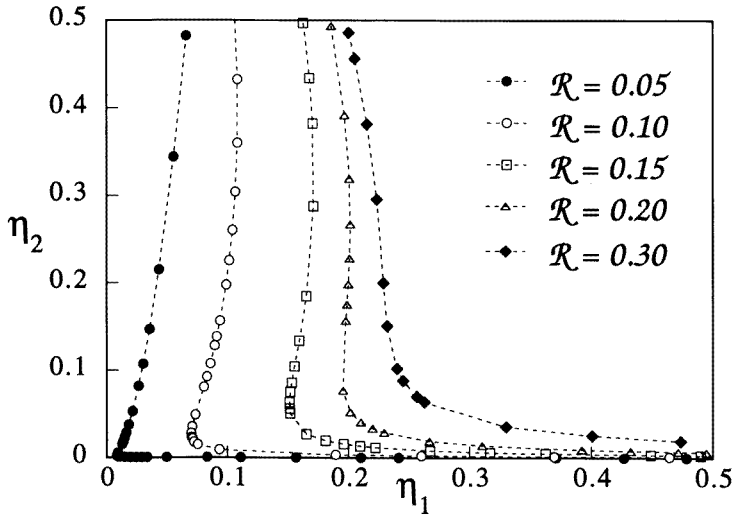

Figure 4. The smaller-sphere packing fraction η_2 plotted as a function of the larger-sphere packing fraction η_1 for five values of the size ratio along the locus of points where $\Delta s(\eta, x_1; \mathcal{R}) = 0$.

of $\mathcal{R}$, the residual multiparticle entropy is positive at all points lying on the right of the curve $\eta_2(\eta_1; \mathcal{R})$. It is rather apparent that such curves have two 'branches': a steeply decreasing one, which corresponds to the lower-concentration portion of the curves shown in figure 3 (i.e., $x_1 \lesssim x_1^{(min)}$), and a rather flat one that is associated with the higher-concentration regime. Furthermore, the first branch shows a re-entrant behaviour for $\mathcal{R} \lesssim 0.2$. In this representation, the larger-sphere packing fraction unveils as a sort of 'order parameter' of the model: in fact, it is only for η_1 greater than a 'critical' value roughly corresponding to the 'knee' of the curve that the mixture starts ordering on a microscopic scale in a way that is manifestly different according to which branch one is considering. In fact, when moving along the steepest branch, η_2 responds in a very sensitive way to small changes of η_1 whose variation remains confined inside a rather thin region. In contrast, along the second branch, η_2 changes very slowly as the larger-sphere mole fraction raises to values which correspond to a denser and denser mixture. The sharp separation between two such regimes fades away with increasing values of the size ratio ($\mathcal{R} \lesssim 0.3$). On the other hand, the systematic shift of the curves with $\mathcal{R}$ towards greater values of η_1 is a clear indication of the lower effectiveness of the osmotic depletion activity exerted by the smaller spheres in competition with thermal disordering effects.

The ordering lines traced through the present entropic criterion are qualitatively similar to the phase-separation boundaries determined by Steiner and co-workers [1] for a system of nearly monodisperse emulsion droplets of two different sizes (see, in particular, figure 2 of [1]). These authors, as well as Imhof and Dhont [2], suggest that phase separation occurs between a fluid and a solid formed by the larger spheres only. Their conclusion is consistent with the present theoretical findings in that the residual multiparticle entropy bridges 'continuously' between the two border situations corresponding to the freezing of the two pure fluids. As far as the quantitative aspects of the calculation are concerned, we recall that, apart from the approximate nature of the current estimate that has been obtained for Δs through its third-order-density expansion, the present criterion usually

anticipates the true phase boundary of the system [15]. Furthermore, as also stressed by Imhof and Dhont [2], the phase lines determined experimentally appear to be very sensitive to even small deviations from the bare hard-sphere behaviour of the model particles used. This fact, together with the sensitivity of different theoretical closures to the nature of the approximations used in the calculations [9–11], makes difficult a truly quantitative comparison between theory and experiment whose mutual agreement remains essentially confined to a qualitative level.

4. Concluding remarks

In this paper we have carried out an analysis of the configurational entropy of a binary hard-sphere mixture in the limit of very low densities. The results confirm the existence of two rather distinct structural regimes which show up for strongly asymmetric sizes and concentrations. In particular, the ordering thresholds traced through the zeros of the residual multiparticle entropy indicate that, upon increasing the concentration of the larger-sphere component, the nature of the transition undergone by the mixture changes in a rather neat way: in fact, the local ordering of the fluid takes place for lower and lower values of the total packing fraction up to a composition beyond which an increase of the larger-sphere mole fraction tends to widen again the disorder region. This behaviour is closely reminiscent of the thermodynamic phenomenology associated with the interplay between the demixing and freezing transitions in a two-component mixture.

Acknowledgments

This work was supported by the Istituto Nazionale per la Fisica della Materia (INFM) and by the Ministero dell'Università e della Ricerca Scientifica e Tecnologica (MURST), Italy.

Appendix. Density expansion of the pair distribution functions

The functions $g_{ij}^{(1)}(r)$ which appear in equation (7) can be expressed as cluster integrals in the form

$$g_{ij}^{(1)}(r_{12}) = \sum_{k=1}^{2} x_k \int f_{ik}(r_{13}) f_{kj}(r_{32}) \, \mathrm{d}\boldsymbol{r}_3 \tag{A1}$$

where $f_{ij}(r) = \exp[-\beta u_{ij}(r)] - 1$ are the Mayer functions. For a mixture of hard-core particles the integral in equation (A1) represents the region of space that is excluded by two spheres centred at $\boldsymbol{r}_1$ and $\boldsymbol{r}_2$ to the centre of a third sphere located in $\boldsymbol{r}_3$. We then get

$$g_{11}^{(1)}(r) = x_1 \mathcal{A}(r) + (1 - x_1)\mathcal{C}(r) \tag{A2}$$

$$g_{12}^{(1)}(r) = x_1 \mathcal{D}(r) + (1 - x_1)\mathcal{E}(r) \tag{A3}$$

$$g_{22}^{(1)}(r) = x_1 \mathcal{C}(r) + (1 - x_1)\mathcal{B}(r) \tag{A4}$$

with

$$\mathcal{A}(r) = \frac{4}{3}\pi\sigma_{11}^3 \left[1 - \frac{3}{4}\frac{r}{\sigma_{11}} + \frac{1}{16}\left(\frac{r}{\sigma_{11}}\right)^3\right]\Theta(2\sigma_{11} - r) \tag{A5}$$

$$\mathcal{B}(r) = \frac{4}{3}\pi\sigma_{22}^3 \left[1 - \frac{3}{4}\frac{r}{\sigma_{22}} + \frac{1}{16}\left(\frac{r}{\sigma_{22}}\right)^3\right]\Theta(2\sigma_{22} - r) \tag{A6}$$

$$\mathcal{C}(r) = \frac{4}{3}\pi\sigma_{12}^3\left[1 - \frac{3}{4}\frac{r}{\sigma_{12}} + \frac{1}{16}\left(\frac{r}{\sigma_{12}}\right)^3\right]\Theta(2\sigma_{12} - r) \tag{A7}$$

$$\begin{aligned}\mathcal{D}(r) = \Bigg\{&\pi\sigma_{11}\left[\sigma_{11} - \sigma_{11}\left(\frac{r^2 + \sigma_{11}^2 - \sigma_{12}^2}{2r\sigma_{11}}\right)\right]^2 - \frac{\pi}{3}\left[\sigma_{11} - \sigma_{11}\left(\frac{r^2 + \sigma_{11}^2 - \sigma_{12}^2}{2r\sigma_{11}}\right)\right]^3 \\ &+ \pi\sigma_{12}\left[\sigma_{12} - \sigma_{12}\left(\frac{r^2 + \sigma_{12}^2 - \sigma_{11}^2}{2r\sigma_{12}}\right)\right]^2 \\ &- \frac{\pi}{3}\left[\sigma_{12} - \sigma_{12}\left(\frac{r^2 + \sigma_{12}^2 - \sigma_{11}^2}{2r\sigma_{12}}\right)\right]^3\Bigg\}\Theta(\sigma_{11} + \sigma_{12} - r)\end{aligned} \tag{A8}$$

$$\begin{aligned}\mathcal{E}(r) = \Bigg\{&\pi\sigma_{12}\left[\sigma_{12} - \sigma_{12}\left(\frac{r^2 + \sigma_{12}^2 - \sigma_{22}^2}{2r\sigma_{12}}\right)\right]^2 - \frac{\pi}{3}\left[\sigma_{12} - \sigma_{12}\left(\frac{r^2 + \sigma_{12}^2 - \sigma_{22}^2}{2r\sigma_{12}}\right)\right]^3 \\ &+ \pi\sigma_{22}\left[\sigma_{22} - \sigma_{11}\left(\frac{r^2 + \sigma_{22}^2 - \sigma_{12}^2}{2r\sigma_{22}}\right)\right]^2 \\ &- \frac{\pi}{3}\left[\sigma_{22} - \sigma_{22}\left(\frac{r^2 + \sigma_{22}^2 - \sigma_{12}^2}{2r\sigma_{22}}\right)\right]^3\Bigg\}\Theta(\sigma_{22} + \sigma_{12} - r)\end{aligned} \tag{A9}$$

where $\Theta(r)$ is the Heaviside step function.

When the diameters of the two species become equal ($\mathcal{R} = 1$), the first-order expressions for the radial distribution functions $g_{ij}^{(1)}(r)$ reduce to those of the one-component case [23].

References

[1] Steiner U, Meller A and Stavans J 1995 *Phys. Rev. Lett.* **74** 4750
[2] Imhof A and Dhont J K G 1995 *Phys. Rev. Lett.* **75** 1662
[3] Frenkel D and Louis A A 1992 *Phys. Rev. Lett.* **68** 3363
[4] Dijkstra M and Frenkel D 1994 *Phys. Rev. Lett.* **72** 298
[5] Dijkstra M, Frenkel D and Hansen J-P 1994 *J. Chem. Phys.* **101** 3179
[6] Cuesta J A 1996 *Phys. Rev. Lett.* **76** 3742
[7] Biben T and Hansen J-P 1991 *Phys. Rev. Lett.* **66** 2215; 1991 *J. Phys.: Condens. Matter* **3** F65
[8] Caccamo C and Pellicane G 1996 *Physica* A at press
[9] Rosenfeld Y 1994 *Phys. Rev. Lett.* **72** 3831
[10] Lekkerkerker H N W and Stroobants A 1993 *Physica* A **195** 387
[11] Amokrane S and Regnaut C 1996 *Phys. Rev.* E **53** 1990
[12] Lee L and Levesque D 1973 *Mol. Phys.* **26** 1351
[13] Fries P H and Hansen J-P 1983 *Mol. Phys.* **48** 891
[14] Barosová M, Malijevský M, Labík S and Smith W R 1996 *Mol. Phys.* **87** 324
[15] Saija F, Giaquinta P V, Giunta G and Prestipino Giarritta S 1994 *J. Phys.: Condens. Matter* **6** 9853
[16] Boublík T and Nezbeda I 1986 *Collect. Czech. Chem. Commun.* **51** 2301
[17] Saija F, Fiumara G and Giaquinta P V 1996 *Mol. Phys.* **87** 991
[18] Hirschfelder J O, Curtiss C F and Bird R B 1966 *Molecular Theory of Gases and Liquids* (New York: Wiley)
[19] Giaquinta P V and Giunta G 1992 *Physica* A **187** 145
[20] Saija F, Fiumara G and Giaquinta P V 1996 *Mol. Phys.* **88** at press
[21] Boublík T 1970 *J. Chem. Phys.* **53** 471
[22] Mansoori G A, Carnahan N F, Starling K E and Leland T W 1971 *J. Chem. Phys.* **54** 1523
[23] Kirkwood J G 1935 *J. Chem. Phys.* **3** 300